



HAL
open science

Mechanistically mapping near-surface temperature in the understory of temperate forests: A validation of the microclima R package against empirical observations

Théo Brusse, Jonathan Lenoir, Nicolas Boisset, Fabien Spicher, Frédéric Dubois, Gaël Caro, Ronan Marrec

► To cite this version:

Théo Brusse, Jonathan Lenoir, Nicolas Boisset, Fabien Spicher, Frédéric Dubois, et al.. Mechanistically mapping near-surface temperature in the understory of temperate forests: A validation of the microclima R package against empirical observations. *Agricultural and Forest Meteorology*, 2024, 346, pp.109894. 10.1016/j.agrformet.2024.109894 . hal-04442818

HAL Id: hal-04442818

<https://hal.science/hal-04442818>

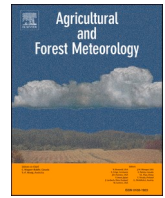
Submitted on 6 Feb 2024

HAL is a multi-disciplinary open access archive for the deposit and dissemination of scientific research documents, whether they are published or not. The documents may come from teaching and research institutions in France or abroad, or from public or private research centers.

L'archive ouverte pluridisciplinaire **HAL**, est destinée au dépôt et à la diffusion de documents scientifiques de niveau recherche, publiés ou non, émanant des établissements d'enseignement et de recherche français ou étrangers, des laboratoires publics ou privés.



Distributed under a Creative Commons Attribution - NonCommercial - NoDerivatives 4.0 International License



Mechanistically mapping near-surface temperature in the understory of temperate forests: A validation of the *microclima* R package against empirical observations

Théo Brusse^{a,b,*}, Jonathan Lenoir^a, Nicolas Boisset^a, Fabien Spicher^a, Frédéric Dubois^a, Gaël Caro^{b,1}, Ronan Marrec^{a,1}

^a UMR CNRS 7058, "Ecologie et Dynamique des Systèmes Anthropisés" (EDYSAN), Université de Picardie Jules Verne, Amiens, France

^b UMR INRAE 1121, "Laboratoire Agronomie Environnement" (LAE), Université de Lorraine, Vandœuvre-les-Nancy, France

ARTICLE INFO

Keywords:

Climate change
Forest microclimates
Mechanistic models
Temperature loggers
Vegetation cover

ABSTRACT

Temperature conditions matter for ground-dwelling biodiversity. However, contrary to ambient-air temperatures as measured by weather stations, there is no global network available yet for measuring microclimate temperatures as perceived by organisms living near the ground. To predict microclimate temperatures near the ground, mechanistic models have been recently developed. Here, we aim at testing the ability of the *microclima* package in R to make mechanistic predictions of real temperature conditions near the ground. Focusing on a network of 45 temperature loggers measuring hourly air temperature near the ground (1-m height) inside and outside the forest of Compiègne, in northern France, we generated hourly maps of near-ground air temperature, as predicted by the *microclima* package, covering the exact same period: February 2018 to October 2019. Our results show a strong correlation between hourly temperatures as predicted by the model and hourly temperatures as measured by loggers ($R^2 = 0.88$). We also found that vegetation height and the Normalized Difference Vegetation Index (NDVI) influence the root mean square error (RMSE) as well as the slope coefficient between measured and predicted temperatures. For instance, increasing vegetation height reduces the RMSE and the slope coefficient between measured and predicted temperatures. Sensors placed in open habitats outside the forest or under low forest canopy height tended to measure higher temperatures than those predicted by the model. Because sensors placed outside forests are likely biased by overheating due to incoming solar radiation, the predictive accuracy of the *microclima* model cannot be quantified in a fair manner. Better and more in-situ data outside forests are needed. Alternatively, the *microclima* package could be tailored to mimic sensor overheating and better reflect the temperature as measured by sensors near the ground in open conditions—(e.g., 3D structure of the vegetation, sliding window approach).

1. Introduction

The activity and distribution of ground-dwelling organisms is strongly determined by temperature conditions near the ground surface (Woods et al., 2015). Depending on vegetation cover and the vertical layering of vegetation as well as terrain complexity, atmospheric conditions, such as ambient-air temperature, can be dramatically altered into a myriad of diverse microclimate conditions—i.e., the conditions that ground-dwelling organisms actually experience—that strongly deviate from the macroclimatic context (Lembrechts et al., 2019).

Forests are an excellent illustration of this, and their role in buffering the macroclimate, especially temperature near the ground, is well known (De Frenne et al., 2019). Microclimate temperature can be defined as the temperature as perceived by organisms inside their proximal habitats, such as the soil-air interface for ground-dwelling insects in grasslands or inside tree holes for forest-dwelling organisms living in dendro-microhabitats (Scheffers et al., 2014). Indeed, there is often an offset between these microclimatic temperatures and the macroclimate temperatures as measured by weather stations (De Frenne et al., 2021), linked to the influence of vegetation cover. Considering the importance

* Corresponding author at: 33 rue St-Leu, 80000 Amiens, France.

E-mail address: theobrusse52@gmail.com (T. Brusse).

¹ These authors have contributed equally to this work.

of temperature conditions on biodiversity living near the ground and below the forest canopy, it is essential to be able to model its temporal variation in a spatially explicit manner to improve our understanding of distribution patterns of living organisms, especially in the context of current climate change (De Frenne et al., 2021).

Collecting microclimate temperature data in space and time can be achieved using temperature loggers placed directly within the microhabitat of the target species (Pincebourde and Salle, 2020). Various types of low-cost temperature loggers exist (e.g., iButton, HOBO Pendant, TMS4, Lascars, etc.), each with measurement capabilities potentially dependent on the habitat type and its direct exposure to solar radiation (Ashcroft, 2018; Maclean et al., 2021; Terando et al., 2017). However, deploying a network of temperature loggers in the field has several limitations in terms of: (i) the spatial extent one can cover; (ii) the spatial heterogeneity of microclimate conditions one can cover inside the focal habitat; and (iii) the logistic costs to maintain such a network of loggers in the long term (Lembrechts et al., 2021a). Besides these technical limitations, one then needs to spatially interpolate temperature conditions as measured by temperature loggers in order to generate spatially contiguous maps of microclimate temperatures inside the focal habitat. For instance, Lembrechts et al. (2020) first established the SoilTemp database storing microclimate temperature data from all over the world before interpolating, using a machine learning approach, soil temperature conditions at 1 km resolution worldwide (Lembrechts et al., 2021b). However, temporal and spatial resolutions of such global maps of soil temperature remain too coarse for local studies. To fill this gap, the most recent microclimate research developed maps of sub-canopy air temperature at 25-m resolution across Europe (Haesen et al., 2023, 2021). In addition, and in parallel to these statistical approaches to map microclimate temperatures at increasingly finer spatiotemporal resolutions, mechanistic models have been recently developed to map microclimate temperature anywhere and at any time from physical mechanisms and without the need for in-situ measurement data. (Lembrechts and Lenoir, 2020; Maclean, 2020).

Maclean et al. (2019) developed the *microclima* R package, a mechanistic model to downscale temperature conditions near the ground. The model can estimate microclimate temperatures at fine spatiotemporal resolutions by relying on ambient-air temperature as measured by weather stations, as well as multiple environmental variables that are known to alter temperature conditions as measured by weather stations. Wind speed and direct solar radiation are the two main atmospheric parameters likely to be reduced in ecosystems with denser and higher vegetation, leading to a dampening of air and soil temperature variations (Gril et al., 2023; Vinod et al., 2023). Microclimate temperatures can deviate from macroclimate temperatures due to various factors. Topographical factors such as elevation and topographic incline have been shown to influence microclimate (e.g., Macek et al., 2019; Rita et al., 2021). For example, high elevations tend to experience cooler temperatures and increased wind speeds compared to low elevations. Similarly, south-facing slopes tend to be warmer and drier than north-facing slopes. Additionally, forests can regulate macroclimate temperatures through vegetation characteristics such as canopy density (Lenoir et al., 2017; Zellweger et al., 2019) and vegetation height (Song et al., 2013). In general, vegetation characteristics and proxies of aboveground biomass, such as the Normalized Difference Vegetation Index (NDVI), are good candidate variables to explain microclimate temperatures (Duffy et al., 2021). For instance, we expect a positive relationship between the buffering effect of vegetation and NDVI, such that higher NDVI values (i.e., denser vegetation) causes a stronger buffering effect of air temperature conditions near the ground. Thus, microclimate temperatures are less variable through time under well-developed vegetation cover (Yue et al., 2007).

Maclean et al. (2019) depicted the *microclima* model as effective and adaptable to various ecosystems, which has been further demonstrated in several studies focusing on: (i) island and coastal ecosystems (Gardner et al., 2021; Maclean et al., 2019); (ii) grassland ecosystems

(Atkin-Willoughby et al., 2022); or (iii) Arctic wetland ecosystems (Deschamps et al., 2022). For instance, Maclean et al. (2019) tested the validity of their model predictions against empirical data from temperature loggers installed in a coastal ecosystem (i.e., heathland system) and found an R^2 of 0.909 and an RMSE of 1.61 °C. However, to our knowledge, no study has attempted yet to compare temperatures as predicted by the *microclima* model with field-measured temperature data inside the understory of temperate forests. As more and more researchers consider using mechanistic approaches to map spatial and temporal variation of microclimate, it is therefore necessary to know if the *microclima* model is also valid in forest ecosystems where the buffering effect of microclimate is particularly pronounced.

In this study, we aim to (i) assess the ability of the *microclima* model developed by Maclean et al. (2019) to reliably predict air temperature conditions near the ground and inside the understory of a temperate forest and (ii) investigate the environmental factors that could explain part of the variation we observed in the strength of the coupling between temperature measurements from the loggers and temperature predictions from the *microclima* model. To achieve this, we worked in a forest located in northern France (the Compiègne forest) and validated the hourly temperature maps generated by the *microclima* package in R through comparison with empirical data acquired by a network of temperature loggers recording during the period 2018–2019.

2. Materials and methods

2.1. Study area

The study was conducted in the temperate deciduous forest of Compiègne (49°17′–49°27′N; 2°45′–3°2′E; 32–148 m altitude) and its surroundings open habitats for comparative purposes (Fig. 1). The forest of Compiègne is a state forest of 144 km² located in northern France and managed by the *Office national des forêts* (ONF). The climate is sub-oceanic with mean annual temperature being 11.3 °C and total annual precipitation being 732 mm, on average, during the 1999–2021 period. The forest of Compiègne is dominated by common beech (*Fagus sylvatica* L.), oak (*Quercus robur* L., *Q. petraea* Liebl.), and Scots pine (*Pinus sylvestris* L.) (ONF, 2012).

2.2. Microclimate data

2.2.1. Microclimate measurements

Forty-five air temperature loggers (HOBO Pendant, UA-001-8, accuracy at 0 to +50 °C: ±0.53 °C) have been installed from February 1st 2018 to August 31st 2019 in the state forest of Compiègne and its surroundings, including forty-one inside the forest (three of which are close to water bodies) and four outside, in open habitats around the forest (Fig. 1). The positions of the loggers inside the forest were determined *a priori* from an environmental sampling strategy that optimizes the variation in environmental conditions (see Table S1 for details of all the variables considered) (Hattab et al., 2017). In short, we first generated a large set of LiDAR-derived variables obtained from an airborne LiDAR flight operated in 2014 and then conducted a multivariate analysis to capture the greatest amount of variation, in terms of vegetation structure and light conditions throughout the forest of Compiègne, within the environmental space reduced to the two or three first principal components. Once we obtained this reduced environmental space characterizing the variation of vegetation structure throughout the forest, we conducted a systematic sampling across this environmental space in order to capture the full range of variation as captured by the airborne LiDAR flight and to obtain a representative sample of the forest. Finally, we projected back our sample in the geographical space which explain why some loggers are located far apart while others are closer to each other (see blue dots in Fig. 1(c)). Note that loggers can be installed in adjacent management units which are homogeneous in themselves but often very different from one another. The microclimatic temperature

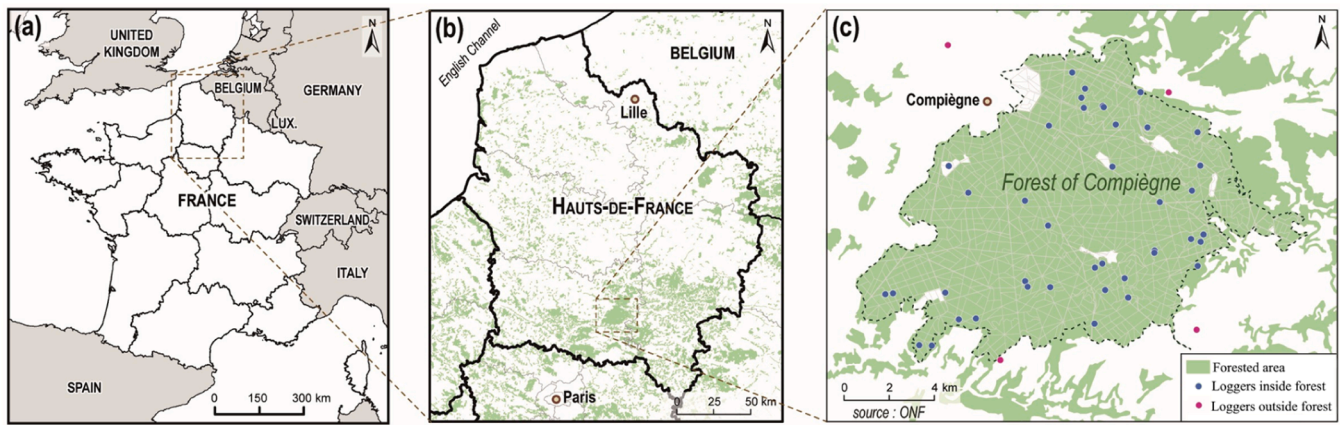


Fig. 1. Localization of (a) the study region in France, (b) the study area inside the study region, and (c) the temperature loggers inside the state forest of Compiègne (41 blue dots) and its surroundings (four red dots) (for interpretation of the references to colour in this figure legend, the reader is referred to the web version of this article).

measured by the sensor is generally only characteristic of the few meters surrounding it (Gril et al., 2023). In addition, we also installed four temperature loggers outside the forest, in fully open conditions to obtain a contrast and assess the predictive accuracy of the *microclima* model in an open environment. These four loggers were installed all around the forest of Compiègne to be representative of the study area (see red dots in Fig. 1(c)).

All temperature sensors were hanging at 1-meter height above ground and attached either on a tree trunk for sensors inside the forest or on a wooden pole for sensors outside the forest. To limit direct sunlight and overheating in response to light radiations, sensors were systematically facing north and were shielded in white homemade PVC tubes ($\varnothing = 10$ cm, $l = 15$ cm) (See Zellweger et al., 2019 for the shielding design we used). The loggers recorded air temperatures at hourly resolution over the entire study period.

2.2.2. Microclimate predictions

Using the mechanistic microclimate model called *microclima* and implemented within R (see Maclean et al., 2019 for a description of the *microclima* package and for more information on how the underlying mechanistic model works), we predicted air temperature conditions near the ground (at 1-m height) at hourly resolution and over the same time period as the period covered by our 45 temperature loggers. We used a large set of variables to calculate the maps of microclimate predictions (Table 1). First, from the input digital elevation model (DEM), the *microclima* model generates a map of the topographic incline to incorporate the effect of topography on microclimate processes. Then, among the other input data needed to run *microclima*, we provided information on vegetation heights across the study area using either literature data or data acquired by the Global Ecosystem Dynamics Investigation (GEDI) satellite (see Table 1). For the area outside the forest of Compiègne we provided monthly maps of vegetation heights to account for height changes related to crop phenology over the studied period (information coming from literature review and agricultural technical institutes; Table S2). For the 41 other sites located inside the forest of Compiègne, map of forest canopy height, as measured in 2019 by the GEDI satellite, was incorporated in the *microclima* model and considered stable over the study period. For vegetation height in the forest, we chose to use GEDI data rather than our airborne LiDAR because of the temporal mismatch between the LiDAR flight operated in 2014 and our study period (2018–2019) and because forest management practices may have severely altered canopy height in several forest management units between 2014 and 2018. In addition to vegetation height and to also capture phenological changes inside the forest that cannot be captured through changes in canopy height, we used monthly

Table 1

List of all variables used to run the *microclima* model.

Input data	Spatial resolution (m)	Temporal resolution	Source
Elevation	25	NA	IGN (https://geoservices.ign.fr/)
NDVI	20	monthly	Copernicus - Sentinel-2 (https://scihub.copernicus.eu/)
Forest height	30	NA	Global Ecosystem Dynamics Investigation (https://glad.umd.edu/dataset/gedi)
Crop height	20	monthly	Literature
2 m temperature	9000	hourly	ERA-5 (https://cds.climate.copernicus.eu/cdsapp#!/dataset/reanalysis-era5-land?tab=overview)
2 m Relative humidity	9000	hourly	
10 m u/v-components of wind	9000	hourly	
Surface pressure	9000	hourly	
Cloud cover	9000	hourly	
Surface solar radiation downwards	9000	hourly	

data on NDVI as an additional input data to run the *microclima* model. We retained only one set of Sentinel-2 images per month with less than 25 % cloud cover to compute NDVI (13 months with NDVI images over the 16-month of the study period). Based on these input data on vegetation characteristics, the *microclima* model generates monthly data related to the effect of vegetation cover on microclimate processes, including surface albedo, fractional canopy cover and the ratio of vertical to horizontal projections of leaf foliage. Finally, the model combines all these variables related to the effect of vegetation cover on microclimate processes (i.e., surface albedo, fractional canopy cover and the ratio of vertical to horizontal projections of leaf foliage, all at 20-m resolution) with the variables describing topography (i.e., topographic incline and elevation). It also includes several layers of weather data available at relatively coarse spatial resolution (9 km \times 9 km) across the entire study area (inside and outside the forest of Compiègne) but at a fine temporal resolution (hourly) to calculate the net radiation as the difference between shortwave and longwave radiation (longwave radiations being previously calculated by the model from meteorological data). From net radiation, the model generates hourly temperature maps from February 2018 to August 2019, with a spatial resolution of 20 m (see Fig. 2 for an example of hourly output on August 15th 2018 at 3:00

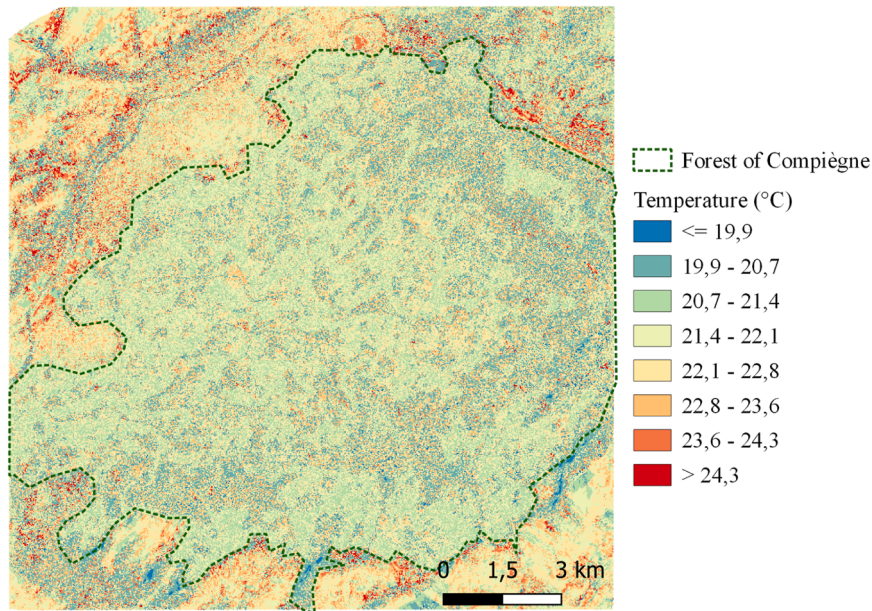


Fig. 2. Example of output map of near-surface air temperature (°C) generated by the microclima model at 20-m resolution across the forest of Compiègne and its surroundings, as of August 15th, 2018 at 3:00 pm. See Fig. S1 for a colorblind friendly version of this figure.

pm).

2.3. Model validation

To assess the quality of the predictions from the mechanistic model implemented in the *microclima* R package, we compared hourly temperature predictions at a given logger location to the corresponding hourly temperature measurements from the focal logger, covering the entire period from February 1st 2018 to August 31st 2019. The strength of the relationship or coupling between predicted and measured hourly temperatures was first assessed for all loggers combined using a linear mixed-effects model (LMM) with the logger ID as a random intercept term to account for the fact that the data are not independent and to deal with the structure of longitudinal data (cf. time series of temperature values for each logger separately).

In addition to the LMM that we fitted across all loggers to get an overall idea of the strength of the coupling between mechanistic predictions and independent empirical measurements in the field, we also assessed the strength of the coupling between predicted and measured hourly temperatures throughout the entire study period but for each logger separately and independently, using a linear modelling (LM) approach (i.e., one LM per logger). We extracted the slope coefficient of the relationship but for each logger separately (i.e., one slope coefficient value per LM) and calculated the corresponding R^2 and the Root Mean

RMSE values. Then, in order to explain the observed variation in the monthly resolution of the slope coefficient and the R^2 and RMSE values (i.e., our set of response variables), we built several models, using a LMM approach with logger ID as a random intercept term (see Eq. (1)), with a set of environmental variables (i.e., vegetation height, NDVI, elevation, and topographic incline) used as explanatory variables for the level of coupling between observed and mechanistically predicted values (i.e., as captured by the slope coefficient and R^2 and RMSE values). We first verified the absence of strong pairwise correlation ($r < 0.5$) between the set of environmental predictor variables, using a Spearman correlation test, and then verified the absence of multicollinearity between the variables (using the variance inflation factor: $VIF < 5$). In addition to vegetation height, NDVI, elevation and topographic incline, we also tested the effect of seasonality by adding “season” as a predictor variable interacting with NDVI (see Eq. (1)). To assess seasonality effect, we considered a factor variable with four levels: winter (total of 4 months: February 2018, December 2018, January 2019, and February 2019); spring (total of 6 months: March 2018 to May 2018 and March 2019 to May 2019); summer (total of 6 months: June 2018 to August 2018 and June 2019 to August 2019); and autumn (total of 3 months: September 2018 to November 2018). Differences in the level of correlation between predicted and observed temperatures across the four seasons were assessed by a Tukey post-hoc test.

$$\text{RMSE}/R^2/\text{slope} \sim \text{poly}(\text{NDVI}, 2) \times \text{season} + \text{poly}(\text{vegetation height}, 2) + \text{poly}(\text{elevation}, 2) + \text{poly}(\text{topographic incline}, 2) + (1|\text{loggers.ID}) \quad (1)$$

Square Error (RMSE) associated with each logger. The RMSE is recognized as an appropriate index to represent model performance for Gaussian data like temperature (Chai and Draxler, 2014). Then, to assess the seasonal signal in the coupling between mechanistic predictions and independent empirical measurements, we repeated the exact same procedure but running a LM for each month and each logger separately. We did not fit a LM for the months when there were logger failures, leading to a total of 630 slope coefficient values, 630 R^2 values, and 630

An interaction term was set between the NDVI and season variable, as the NDVI is season dependant. Quadratic effects were inserted into the equation to take into account possible non-linear relationships between each predictors and the focal response variable (RMSE, R^2 or the slope coefficient).

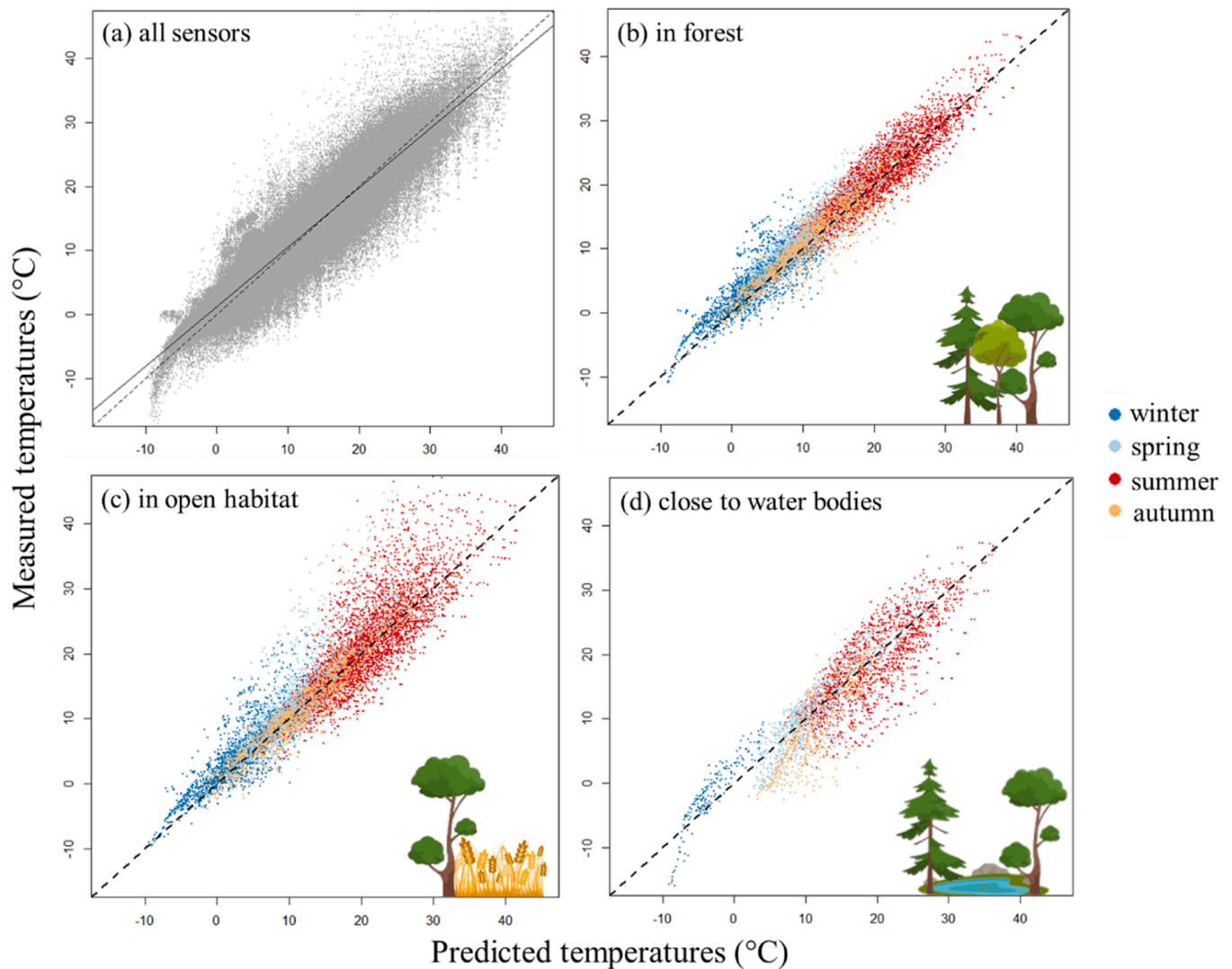


Fig. 3. Correlation between measured and predicted hourly temperatures (mechanistic modelling), for (a) all loggers combined, (b) a logger where measured temperatures are strongly coupled with predicted temperatures, (c) a logger where measured temperatures tend to exceed predicted temperatures, and (d) a logger where measured temperatures tend to be exceeded by predicted temperatures. Dashed line is the identity line and solid line is the regression line.

3. Results

Over the period starting from February 2018 to August 2019, the average temperature measured by all loggers ($n = 45$) was $14.08\text{ }^{\circ}\text{C}$ (standard deviation = $8.08\text{ }^{\circ}\text{C}$) and the average temperature predicted at the same 45 locations by the mechanistic modelling approach used in *microclima* was $13.87\text{ }^{\circ}\text{C}$ (standard deviation = $8.14\text{ }^{\circ}\text{C}$).

All loggers combined ($n = 45$), we found that the strength of the coupling between empirically measured and mechanistically predicted temperatures at an hourly resolution was high with a mean slope coefficient estimate as provided by the LMM of 0.93 (i.e., very close to one or identity), a conditional R^2 value of 0.88 (marginal $R^2 = 0.87$), and an RMSE value of $2.92\text{ }^{\circ}\text{C}$ (Fig. 3(a)). Regarding our LM results based on each logger independently, we noted important variation in the degree of coupling between measured and predicted temperatures, with values ranging from 0.80 to 1.12 for the slope coefficient (mean slope = 0.93), values ranging from 0.78 to 0.94 for the R^2 coefficient (mean $R^2 = 0.88$), and RMSE values ranging from 2.10 to $4.43\text{ }^{\circ}\text{C}$ (mean RMSE = $2.90\text{ }^{\circ}\text{C}$) (see Table S3 in the Supplementary Material for detailed results per logger). On a logger-by-logger basis, most loggers located inside the forest showed a rather good coupling between hourly temperatures as recorded by our loggers and hourly temperatures as predicted by the

microclima model (Fig. 3(b)). Yet, under some circumstances, we noted significant differences and deviations between the empirically measured and mechanistically predicted temperatures (Fig. 3(c) and (d)). For instance, hourly temperature measurements from a logger located in open conditions outside the forest (red dots in Fig. 1(c)) had a tendency to exceed hourly temperatures as predicted by the *microclima* model, especially so during the summer season (red dots in Fig. 3(c)). On the contrary, hourly temperature measurements as predicted by the *microclima* model had a tendency to overestimate hourly temperature as recorded from a logger located near a water body (e.g., a pond) in the forest, especially during the summer season (red dots in Fig. 3(d)).

The level of coupling between empirically measured and mechanistically predicted temperatures varied across the four seasons (Fig. 4). The RMSE value was lower (i.e., best predictive performances), on average, during autumn and winter compared to spring and summer (Fig. 4(a)). The R^2 value was higher (i.e., higher explanatory power of mechanistically predicted temperatures), on average, during autumn compared to other seasons (Fig. 4(b)). Finally, the slope coefficient was closer to one (i.e., perfect coupling), on average, during spring and winter in comparison to summer and autumn (Fig. 4(c)). Regarding our LMMs to explain the variation we observed in the degree of coupling between empirically measured and mechanistically predicted

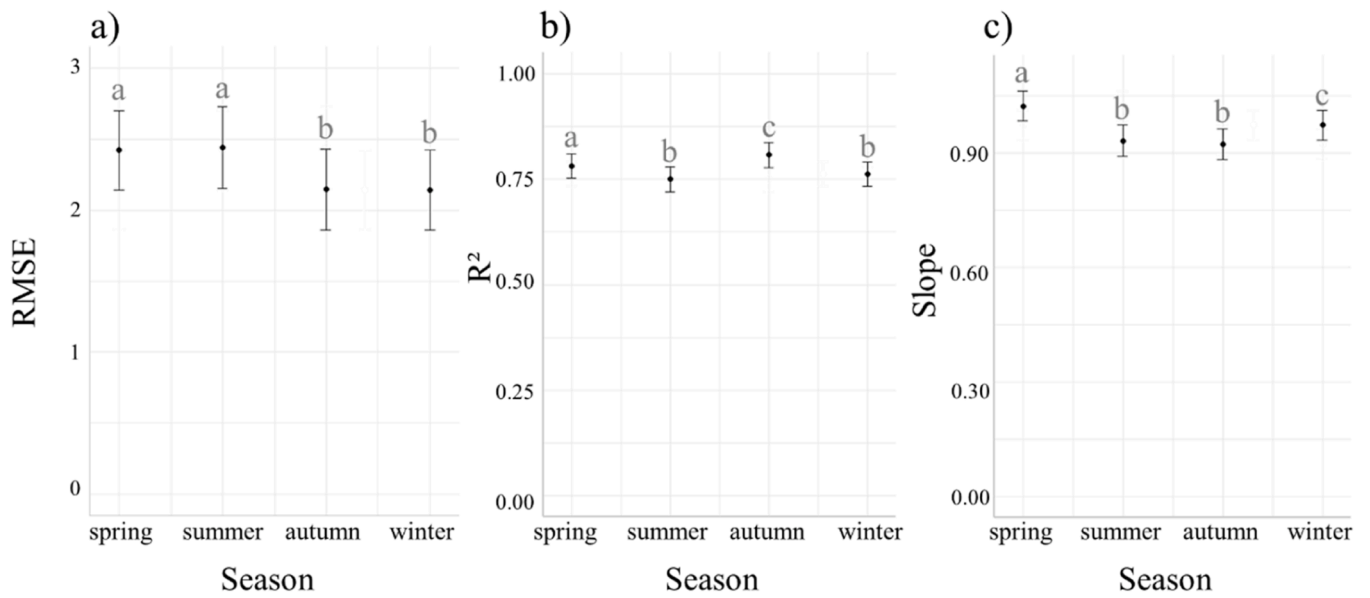


Fig. 4. Mean values of (a) the RMSE, (b) the R^2 , and (c) the slope coefficient of the relationship between empirically measured and mechanistically predicted temperatures, according to season. Error bars represent standard deviation. Different letters between two seasons indicate a significantly different mean estimate of the focal response variable (RMSE, R^2 , or slope coefficient) (p -value < 0.05).

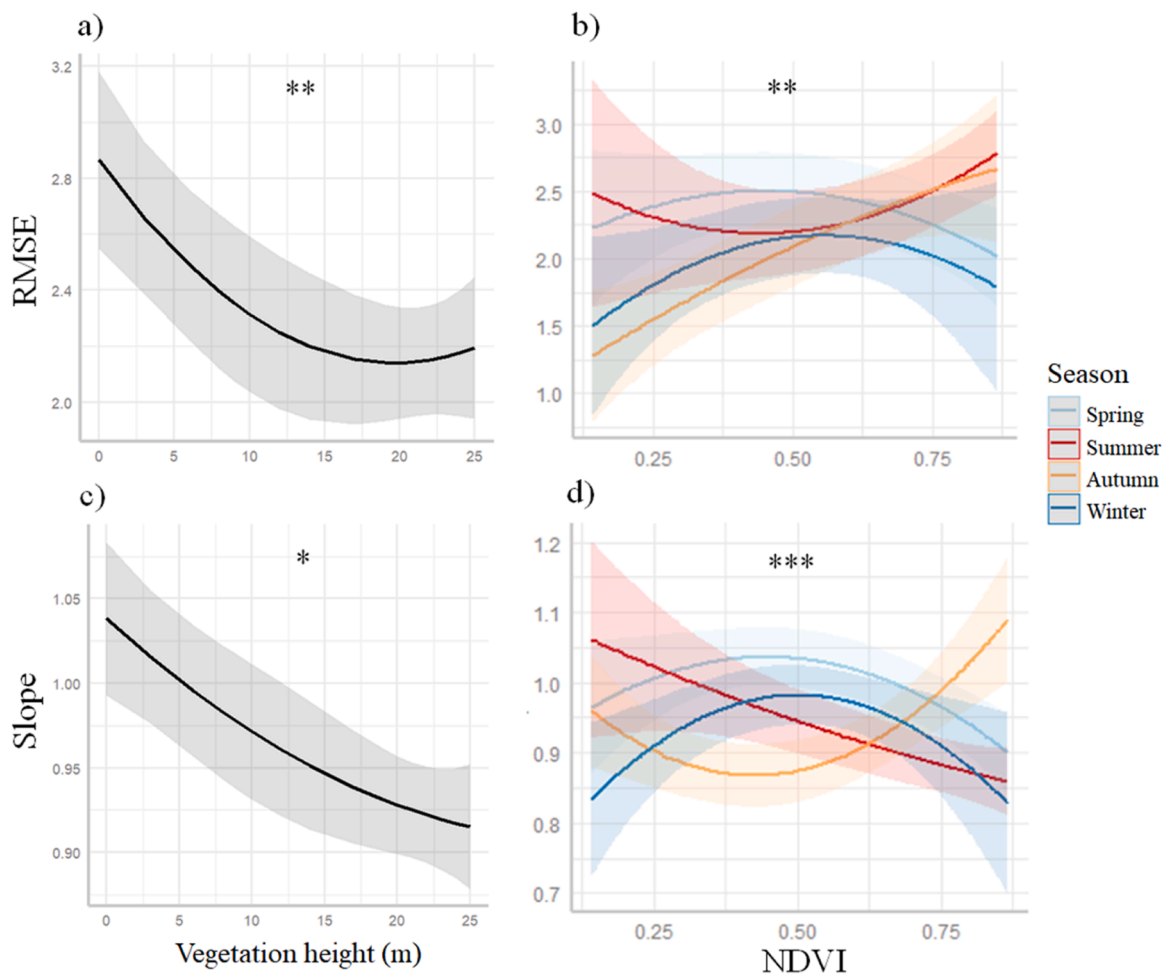


Fig. 5. Impact of environmental variables on the magnitude of the focal response variable extracted from univariate linear model between mechanistically predicted and empirically measured temperatures. Translucent ribbons representing the standard deviation. Symbols: 0.01 < p -value < 0.05 (*); 0.001 < p -value < 0.01 (**); p -value < 0.001 (***).

temperatures, we found that only vegetation height and the interaction effect between NDVI and season had a significant influence on the RMSE value and the slope coefficient (Fig. 5). The RMSE value was negatively correlated with vegetation height, reaching the lowest RMSE values (i.e., best predictive performances) in forest stands with canopies of 15 m or higher. Vegetation height also had a negative effect on the slope coefficient such that the slope coefficient was higher than one (i.e., amplification of extreme values) in low-stature vegetation but lower than one under higher forest canopies (i.e., buffering effect), with the slope coefficient reaching one (i.e., perfect coupling) when vegetation height was around 5 m. The effect of NDVI on the RMSE value and the slope coefficient was altered by the season. We found RMSE reached the lowest values (i.e., best predictive performances) when NDVI was low during autumn and winter, and when NDVI was high during the winter. We also found a negative effect of NDVI on the slope coefficient during summer, such that the slope coefficient was lower than one when aboveground vegetation biomass was high but higher than one when aboveground vegetation biomass was low. In general, the slope coefficient was reaching values close to one (i.e., perfect coupling) at intermediate NDVI values. Finally, the observed variation in the R^2 value was not influenced by any of the variables we tested.

4. Discussion

Overall, our findings suggest that the *microclima* model developed by Maclean et al. (2019) performs relatively well at predicting hourly air temperature near the ground in temperate forest ecosystems. We found a relatively strong level of coupling across all hourly records between the empirically measured and mechanistically predicted temperatures, with a slope coefficient of 0.93 (i.e., close to one) and an overall R^2 value of 0.88. On the other hand, the RMSE of 2.92 °C is high and indicates a low accuracy in the prediction of temperatures near the ground by the *microclima* model. While the coefficient of determination (R^2) is often used to assess the quality of a model, it can be misleading, especially when applied to data with a wide range of values, as is the case with temperatures ranging from -20 °C to +50 °C in our study system. Indeed, a high R^2 value may simply reflect the fact that predicted values are generally close to observed values, without necessarily indicating that the model is accurate. This is where the RMSE comes in, giving a more objective idea of the accuracy of predictions. In our case, the RMSE measures the mean difference between mechanistically predicted and empirically observed values, giving a direct indication of the model's prediction error. So, even if the R^2 is high, a substantial RMSE (close to 3 °C in our case) should not be underestimated, as it indicates a significant error in the model's predictions. This is why it is essential to consider both R^2 and RMSE values when evaluating the performance of a predictive model. In short, while R^2 can be influenced by the range of observed values and is therefore dependent on the study system and temporal resolution, RMSE provides a more robust and objective measure of model accuracy.

We found that the modelling performances of the *microclima* model were the best, in terms of model accuracy (i.e., low RMSE values), during autumn while the level of coupling between predicted and observed temperatures was the best (i.e., slope coefficient close to one) during spring. Most importantly, we found that the RMSE value between the mechanistic predictions from the *microclima* model and our empirical observations across all our loggers was negatively related to vegetation height. This suggests that the *microclima* model performs best, in terms of its accuracy at predicting air temperatures at an hourly interval closest to measurement values, under high forest canopies while its accuracy strongly decreases when canopy height is low, namely in fully open conditions (see Fig. 3(b) and (c) as two opposite extreme examples of loggers located under high canopy and in a fully open site outside the forest of Compiègne). We believe that a high canopy provides more space for several vegetation layers to develop and densify canopy cover than in areas with a low-stature canopy. Thus, solar radiation reaching

the ground is less abundant under high canopies, reducing overheating of temperature sensors and resulting in lower RMSE values. Similarly, we found that the *microclima* model has a tendency to overestimate temperature conditions compared to empirical measurements (i.e., slope coefficient lower than one) under high forest canopies while it tends to underestimate temperature conditions compared to temperatures as recorded by loggers (i.e., slope coefficient higher than one) under low vegetation height and in fully open conditions. This is consistent with former findings suggesting that temperature loggers located outside forests in fully open conditions tend to overheat and thus overestimate the true air temperature (Maclean et al., 2021).

We can observe a tendency of the *microclima* model to underestimate the warmest temperatures, in some conditions. These temperature differences are reflected in the high RMSE value of 2.92 °C we obtained when analysing the loggers altogether. Seasonally, the largest differences were observed during spring and summer. These differences may be due to measurement errors of the loggers' sensors caused by their greater exposure to solar radiation during spring and summer and low air-mixing due to low wind exposure, causing an overheating and thus an overestimation of the measured temperature by the loggers. We used a similar approach to identify variations in correlation levels depending on the time of the day, and also observed a decrease in correlation level for the coldest (i.e., from 1am to 6am) and warmest hours (i.e., from 1pm to 6pm) (Table S4). Congruently, Maclean et al. (2021) found that loggers accuracy in open habitats can be altered by overheating during the warmest periods of the day or year, and overcooling during the coldest periods of the night or year. Then, the authors suggest that their use should be avoided in locations exposed to direct sunlight/moonlight and close to the soil where wind speed can dramatically slow down, limiting air circulation. Additionally, the high RMSE value could also partially be due to the temporal offset between measured and predicted temperatures. Indeed, the minimum and maximum of measured temperatures are reached after the minimum and maximum of predicted temperatures, with a time difference ranging between one and two hours (Fig. S2).

Other results of our study support this view. First, the correlation level between hourly measured and predicted temperatures varies spatially depending on the environmental characteristics of the forest (Fig. 5). We found that the difference between mechanistically predicted and empirically measured temperatures decreased with increasing vegetation height, with the smallest differences observed in areas with vegetation heights of 15 m or more. Some studies found that vegetation height is one of the main factors influencing temperature near the ground, by limiting effects of exposure to direct solar radiation (e.g., Green et al., 1984; Yu et al., 2018) and so limiting the risk of overheating effect from the loggers. Second, in open areas, such as crop fields located near the outer edge of the forest, the correlation level between hourly measured and predicted temperatures was notably lower than in forest stands. However, in our case study, loggers were installed 1 m above the ground, and were thus most of the time above the vegetation canopy in open areas. To better evaluate the accuracy of the model in open ecosystems, it might be more interesting to consider loggers set at the ground surface.

While the *microclima* model can be useful for mechanistically predicting temperature near the ground within forest habitats, it is not without limitations. One major issue is that the model is heavily dependent on the quality of the data that is fed into it. For example, we used GEDI data (satellite-borne LiDAR) to estimate forest vegetation height, but it would be more informative to use airborne LiDAR data whenever available to have a more accurate estimation of vegetation height at an even finer spatial resolution (Lenoir et al., 2022). This problem is especially true for ecosystems with low vegetation height changing rapidly over time (e.g., crops, grasslands). In our study, we took this into account by modelling monthly vegetation height maps in cultivated areas. In addition, in its current implementation, the *microclima* model does not integrate all variables that can alter the

microclimate conditions. For instance, the effects of the vertical complexity of the vegetation structure, in terms of vegetation layering, on understory temperature are not integrated, even though sub-canopy and understory layers are recognized as strong microclimate drivers, and should be included in the *microclima* model for better estimation of temperature near the ground (Kovács et al., 2017; Stickley and Ferrigno, 2021; Gril et al., 2023). This information can reflect the method of forest management and the age of a forest stand, which both alter tree and shrub density as well as the amount of solar radiation reaching the ground (Lindenmayer et al., 2022). Finally, the model does not fully account for the influence of the surrounding landscape when computing the microclimate temperature within each pixel. As such, the model may predict the same time series of understory temperatures towards the edge or the interior of a forest stand if all implemented parameters are otherwise equal. However, it is well-established that an edge-interior temperature gradient exists in forests and forest stands (Meussen et al., 2021), which may not be reflected in NDVI of vegetation heights values as currently implemented in *microclima*. A possible perspective would be to use a sliding window approach to account for landscape effects on microclimate temperatures (Ma et al., 2017).

In terms of prospects, the model's behaviour could be assessed by working on daily temperature aggregates (instead of the hourly temperatures used in the present study). This approach could lead to lower RMSE values because daily aggregates might smooth over potential mismatches between model and data at fine temporal resolution as seen in Fig. S2. Interestingly, while RMSE values would be lower on daily aggregates (i.e., indicating a better accuracy of the model), R^2 values might also be lower, due to the decreased range of temperatures. It should be noted that working on daily aggregates would be sufficient for many applications, such as for ecologists seeking to understand the relationship between biodiversity and microclimate, especially if later on, monthly or yearly means and ranges are to be calculated. Another prospect would be to improve not only the *microclima* model, but also the in-situ measurements. For example, the white PVC tubes we used to protect the loggers may have little capacity to limit overheating effects in open habitats, contrary to our expectations. The accuracy of the measured temperatures could be improved by using a ventilated shelter to limit the overheating effect. So, the dependence of logger's accuracy on solar radiation and wind exposure may partly explain the differences observed in our study between predicted and measured temperatures, for instance in the context of open areas or in places near water. Moreover, using fine-wire thermocouples, which have a better capacity for measuring air temperatures without overheating (Maclean et al., 2021), would make it possible to approach the "absolute truth" in terms of microclimate temperature. Finally, it should be noted that the *microclimc* model, a "sister model", has been tested for its reliability in a forest ecosystem (Maclean and Klings, 2021). This point-based model has made it possible to improve the prediction of below-canopy temperatures on a fine temporal scale, by considering transient processes such as heat and vapour exchange within and below forest canopy. As our particular research question was to provide gridded temperature maps, it would be interesting to incorporate the specificities of *microclimc* in a new model in order to improve the fine-scale spatiotemporal prediction of temperatures under the forest canopy.

5. Conclusion

Our findings support the idea that the *microclima* package in R is an effective mechanistic model for predicting temperatures near the ground in temperate forest habitats. This model considers various factors such as radiation exposure, wind speed, topography, and vegetation characteristics to predict how temperatures vary spatially and temporally across forest stands. By incorporating these factors, the model can predict the temperature gradients that exist within the forest, which are critical for understanding how different species of plants and animals will interact with their environment. Our study thus allows us to better optimize the

modelling of predicted temperatures in more open ecosystems and highlights the need to validate predictions with observed temperature data. Based on our findings, we conclude that the *microclima* model can be safely extended to other temperate forest habitats with high vegetation height that do not have in-situ microclimate measurements data to predict microclimate temperature variations near the ground. However, the capabilities of the *microclima* model to estimate temperatures in open or low-stature vegetation environments is questioned due to the sensitivities of temperature loggers to overheating. There is still a lack of research that focuses on predicting microclimate in open area systems (e.g., crops and grasslands). The use of loggers placed close to the ground, under the crop canopy, especially high-performance fine-wire thermocouples, could reduce this sensitivity to overheating.

Declaration of generative AI and AI-assisted technologies in the writing process

The authors state that they did not use any AI tools to write the text or to analyse and draw insights from data as part of the research process.

CRedit authorship contribution statement

Théo Brusse: Conceptualization, Formal analysis, Investigation, Methodology, Writing – original draft, Writing – review & editing. **Jonathan Lenoir:** Conceptualization, Funding acquisition, Writing – original draft, Writing – review & editing, Resources. **Nicolas Boisset:** Formal analysis, Resources. **Fabien Spicher:** Writing – original draft, Resources. **Frédéric Dubois:** Writing – original draft, Writing – review & editing. **Gaël Caro:** Conceptualization, Supervision, Writing – original draft, Writing – review & editing. **Ronan Marrec:** Conceptualization, Supervision, Writing – original draft, Writing – review & editing.

Declaration of competing interest

The authors declare that they have no known competing financial interests or personal relationships that could have appeared to influence the work reported in this paper.

Data availability

Data will be made available on request.

Acknowledgement

We thank Emilie Gallet-Moron for generating the first figure and for preprocessing and providing the NDVI data. JL acknowledges funding from the Agence Nationale de la Recherche (ANR), under the framework of the collaborative research program funding scheme (Grant no. ANR-21-CE32-0012-03: MaCCMic project) and the young researcher funding scheme (Grant no. ANR-19-CE32-0005-01: IMPRINT project), as well as funding from the A2U consortium (ALLIANcE project). JL also acknowledges the Région Hauts-de-France, the Ministère de l'Enseignement Supérieur et de la Recherche and the European Fund for Regional Economic Development for their financial support to the CPER ECRIN program.

Supplementary materials

Supplementary material associated with this article can be found, in the online version, at [doi:10.1016/j.agrformet.2024.109894](https://doi.org/10.1016/j.agrformet.2024.109894).

References

- Ashcroft, M.B., 2018. Which is more biased: standardized weather stations or microclimatic sensors? *Ecol. Evol.* 8, 5231–5232. <https://doi.org/10.1002/ece3.3965>.
- Atkin-Willoughby, J., Hollick, S., Pritchard, C.E., Williams, A.P., Davies, P.L., Jones, D., Smith, A.R., 2022. Microclimate drives shelter-seeking behaviour in lambing ewes. *Forests* 13, 2133. <https://doi.org/10.3390/f13122133>.
- Chai, T., Draxler, R.R., 2014. Root mean square error (RMSE) or mean absolute error (MAE)?—Arguments against avoiding RMSE in the literature. *Geosci. Model Dev.* 7, 1247–1250. <https://doi.org/10.5194/gmd-7-1247-2014>.
- De Frenne, P., Lenoir, J., Luoto, M., Scheffers, B.R., Zellweger, F., Aalto, J., Ashcroft, M. B., Christiansen, D.M., Decocq, G., De Pauw, K., Govaert, S., Greiser, C., Gril, E., Hampe, A., Jucker, T., Klings, D.H., Koelemeijer, I.A., Lembrechts, J.J., Marrec, R., Meeussen, C., Ogée, J., Tyystjärvi, V., Vangansbeke, P., Hylander, K., 2021. Forest microclimates and climate change: importance, drivers and future research agenda. *Glob. Change Biol.* 27, 2279–2297. <https://doi.org/10.1111/gcb.15569>.
- De Frenne, P., Zellweger, F., Rodríguez-Sánchez, F., Scheffers, B.R., Hylander, K., Luoto, M., Vellend, M., Verheyen, K., Lenoir, J., 2019. Global buffering of temperatures under forest canopies. *Nat. Ecol. Evol.* 3, 744–749. <https://doi.org/10.1038/s41559-019-0842-1>.
- Deschamps, L., Maire, V., Chen, L., Fortier, D., Gauthier, G., Morneau, A., Hardy-Lachance, E., Dalcher-Gosselin, I., Tanguay, F., Gignac, C., McKenzie, J.M., Rochefort, L., Lévesque, E., 2022. Increased nutrient availability speeds up permafrost development, while goose grazing slows it down in a Canadian High Arctic wetland. *J. Ecol.* <https://doi.org/10.1111/1365-2745.14037>.
- Duffy, J.P., Anderson, K., Fawcett, D., Curtis, R.J., Maclean, I.M.D., 2021. Drones provide spatial and volumetric data to deliver new insights into microclimate modelling. *Landscape Ecol.* 36, 685–702. <https://doi.org/10.1007/s10980-020-01180-9>.
- Gardner, A.S., Gaston, K.J., Maclean, I.M.D., 2021. Accounting for inter-annual variability alters long-term estimates of climate suitability. *J. Biogeogr.* 48, 1960–1971. <https://doi.org/10.1111/jbi.14125>.
- Green, F.H.W., Harding, R.J., Oliver, H.R., 1984. The relationship of soil temperature to vegetation height. *J. Climatol.* 4, 229–240. <https://doi.org/10.1002/joc.3370040302>.
- Gril, E., Laslier, M., Gallet-Moron, E., Durrieu, S., Spicher, F., Le Roux, V., Brasseur, B., Haesen, S., Van Meerbeek, K., Decocq, G., Marrec, R., Lenoir, J., 2023. Using airborne LiDAR to map forest microclimate temperature buffering or amplification. *Remote Sens. Environ.* 298, 113820. <https://doi.org/10.1016/j.rse.2023.113820>.
- Haesen, S., Lembrechts, J.J., De Frenne, P., Lenoir, J., Aalto, J., Ashcroft, M.B., Kopecký, M., Luoto, M., Maclean, I., Nijs, I., Niittynen, P., Hoogen, J., Arriga, N., Brúna, J., Buchmann, N., Čiliak, M., Collalti, A., De Lombaerde, E., Descombes, P., Gharun, M., Goded, I., Govaert, S., Greiser, C., Grelle, A., Gruening, C., Hederová, L., Hylander, K., Kreyling, J., Kruijt, B., Macek, M., Mális, F., Man, M., Manca, G., Matula, R., Meeussen, C., Merinero, S., Minerbi, S., Montagnani, L., Muffler, L., Ogaya, R., Penuelas, J., Plichta, R., Portillo-Estrada, M., Schmeddes, J., Shekhar, A., Spicher, F., Ujházyová, M., Vangansbeke, P., Weigel, R., Wild, J., Zellweger, F., Van Meerbeek, K., 2021. ForestTemp—Sub-canopy microclimate temperatures of European forests. *Glob. Change Biol.* 27, 6307–6319. <https://doi.org/10.1111/gcb.15892>.
- Haesen, S., Lembrechts, J.J., De Frenne, P., Lenoir, J., Aalto, J., Ashcroft, M.B., Kopecký, M., Luoto, M., Maclean, I., Nijs, I., Niittynen, P., van den Hoogen, J., Arriga, N., Brúna, J., Buchmann, N., Čiliak, M., Collalti, A., De Lombaerde, E., Descombes, P., Gharun, M., Goded, I., Govaert, S., Greiser, C., Grelle, A., Gruening, C., Hederová, L., Hylander, K., Kreyling, J., Kruijt, B., Macek, M., Mális, F., Man, M., Manca, G., Matula, R., Meeussen, C., Merinero, S., Minerbi, S., Montagnani, L., Muffler, L., Ogaya, R., Penuelas, J., Plichta, R., Portillo-Estrada, M., Schmeddes, J., Shekhar, A., Spicher, F., Ujházyová, M., Vangansbeke, P., Weigel, R., Wild, J., Zellweger, F., Van Meerbeek, K., 2023. FORESTCLIM—Bioclimatic variables for microclimate temperatures of European forests. *Glob. Change Biol.* <https://doi.org/10.1111/gcb.16678>.
- Hattab, T., Garzón-López, C.X., Ewald, M., Skowronek, S., Aerts, R., Horen, H., Brasseur, B., Gallet-Moron, E., Spicher, F., Decocq, G., Feilhauer, H., Honnay, O., Kempeneers, P., Schmidlein, S., Somers, B., Van De Kerchove, R., Rocchini, D., Lenoir, J., 2017. A unified framework to model the potential and realized distributions of invasive species within the invaded range. *Divers. Distrib.* 23, 806–819. <https://doi.org/10.1111/ddi.12566>.
- Kovács, B., Tinya, F., Odor, P., 2017. Stand structural drivers of microclimate in mature temperate mixed forests. *Agric. For. Meteorol.* 234–235, 11–21. <https://doi.org/10.1016/j.agrformet.2016.11.268>.
- Lembrechts, J.J., Aalto, J., Ashcroft, M.B., De Frenne, P., Kopecký, M., Lenoir, J., Luoto, M., Maclean, I.M.D., Rouspard, O., Fuentes-Lillo, E., García, R.A., Pellissier, L., Pitteloud, C., Alatalo, J.M., Smith, S.W., Björk, R.G., Muffler, L., Ratier Backes, A., Cesarz, S., Gottschall, F., Okello, J., Urban, J., Plichta, R., Svátek, M., Phartyal, S.S., Wipf, S., Eisenhauer, N., Púscas, M., Turtureanu, P.D., Varlagin, A., Dimarco, R.D., Jump, A.S., Randall, K., Dorrepaal, E., Larson, K., Walz, J., Vitale, L., Svoboda, M., Finger Higgens, R., Halbritter, A.H., Curasi, S.R., Klupar, I., Kooztz, A., Pearce, W.D., Simpson, E., Stelmkowsky, M., Jessen Graae, B., Vedel Sørensen, M., Høye, T.T., Fernández Calzado, M.R., Lorite, J., Carbonegni, M., Tomaselli, M., Forte, T.G.W., Petraglia, A., Haesen, S., Somers, B., Van Meerbeek, K., Björkman, M. P., Hylander, K., Merinero, S., Gharun, M., Buchmann, N., Dolezal, J., Matula, R., Thomas, A.D., Bailey, J.J., Ghosn, D., Kazakis, G., de Pablo, M.A., Kemppinen, J., Niittynen, P., Rew, L., Seipel, T., Larson, C., Speed, J.D.M., Ardó, J., Cannone, N., Guglielmin, M., Malfasi, F., Bader, M.Y., Canessa, R., Stanisci, A., Kreyling, J., Schmeddes, J., Teuber, L., Aschero, V., Čiliak, M., Mális, F., De Smedt, P., Govaert, S., Meeussen, C., Vangansbeke, P., Gigauri, K., Lamprecht, A., Pauli, H., Steinbauer, K., Winkler, M., Ueyama, M., Nuñez, M.A., Ursu, T.-M., Haider, S., Wedegärtner, R.E.M., Smiljanic, M., Trouillier, M., Wilmking, M., Altman, J., Brúna, J., Hederová, L., Macek, M., Man, M., Wild, J., Vittoz, P., Pärtel, M., Barančok, P., Kanka, R., Kollár, J., Palaj, A., Barros, A., Mazzolari, A.C., Bauters, M., Boeckx, P., Benito Alonso, J.-L., Zong, S., Di Cecco, V., Sitková, Z., Tielbörger, K., van den Brink, L., Weigel, R., Homeier, J., Dahlberg, C.J., Medinets, S., Medinets, V., De Boeck, H.J., Portillo-Estrada, M., Verryck, L.T., Milbau, A., Daskalova, G.N., Thomas, H.J.D., Myers-Smith, I.H., Blonder, B., Stephan, J.G., Descombes, P., Zellweger, F., Frei, E.R., Heinesch, B., Andrews, C., Dick, J., Siebicke, L., Rocha, A., Senior, R.A., Rixen, C., Jimenez, J.J., Boike, J., Pauchard, A., Scholten, T., Scheffers, B., Klings, D., Basham, E.W., Zhang, J., Zhang, Z., Géron, C., Faziolug, F., Candan, O., Sallo Bravo, J., Hrbacek, F., Laska, K., Cremonese, E., Haase, P., Moyano, F.E., Rossi, C., Nijs, I., 2020. SoilTemp: a global database of near-surface temperature. *Glob. Change Biol.* 26, 6616–6629. <https://doi.org/10.1111/gcb.15123>.
- Lembrechts, J.J., Lenoir, J., 2020. Microclimatic conditions anywhere at any time! *Glob. Change Biol.* 26, 337–339. <https://doi.org/10.1111/gcb.14942>.
- Lembrechts, J.J., Lenoir, J., Scheffers, B., De Frenne, P., 2021a. Designing countrywide and regional microclimate networks. *Glob. Ecol. Biogeogr.* 30, 1168–1174. <https://doi.org/10.1111/gcb.13290>.
- Lembrechts, J.J., Nijs, I., Lenoir, J., 2019. Incorporating microclimate into species distribution models. *Ecography* 42, 1267–1279. <https://doi.org/10.1111/ecog.03947>.
- Lembrechts, J.J., van den Hoogen, J., Aalto, J., Ashcroft, M.B., De Frenne, P., Kemppinen, J., Kopecký, M., Luoto, M., Maclean, I.M.D., Crowther, T.W., Bailey, J. J., Haesen, S., Klings, D.H., Niittynen, P., Scheffers, B.R., Van Meerbeek, K., Aartsma, P., Abdalaze, O., Abedi, M., Aerts, R., Ahmadian, N., Ahrends, A., Alatalo, J.M., Alexander, J.M., Nina Allonsius, C., Altman, J., Ammann, C., Andres, C., Andrews, C., Ardó, J., Arriga, N., Arzac, A., Aschero, V., Assis, R.L., Johann Assmann, J., Bader, M.Y., Bahalkeh, K., Barančok, P., Barrio, I.C., Barros, A., Barthel, M., Basham, E.W., Bauters, M., Bazzichetto, M., Bellelli Marchesini, L., Bell, M.C., Benavides, J.C., Luis Benito Alonso, J., Berauer, B.J., Bjerke, J.W., Björk, R.G., Björkman, M.P., Björnsdóttir, K., Blonder, B., Boeckx, P., Boike, J., Bokhorst, S., Brum, B.N.S., Brúna, J., Buchmann, N., Buysse, P., Luís Camargo, J., Campoe, O.C., Candan, O., Canessa, R., Cannone, N., Carbonegni, M., Carnicer, J., Casanova-Katny, A., Cesarz, S., Chojnicki, B., Choler, P., Chown, S.L., Cifuentes, E.F., Čiliak, M., Contador, T., Convey, P., Cooper, E.J., Cremonese, E., Curasi, S.R., Curtis, R., Cutini, M., Johan Dahlberg, C., Daskalova, G.N., Angel de Pablo, M., Della Chiesa, S., Dengler, J., Deronde, B., Descombes, P., Di Cecco, V., Di Musciano, M., Dick, J., Dimarco, R.D., Dolezal, J., Dorrepaal, E., Dušek, J., Eisenhauer, N., Eklundh, L., Erickson, T.E., Erschbamer, B., Eugster, W., Ewers, R.M., Exton, D.A., Fanin, N., Faziolug, F., Feigenwinter, J., Fenu, G., Ferlian, O., Rosa Fernández Calzado, M., Fernández-Pascual, E., Finckh, M., Finger Higgens, R., Forte, T.G.W., Freeman, E.C., Frei, E.R., Fuentes-Lillo, E., García, R.A., García, M.B., Géron, C., Gharun, M., Ghosn, D., Gigauri, K., Gobin, A., Goded, I., Goekede, M., Gottschall, F., Goulding, K., Govaert, S., Jessen Graae, B., Greenwood, S., Greiser, C., Grelle, A., Guénard, B., Guglielmin, M., Guillemot, J., Haase, P., Haider, S., Halbritter, A.H., Hamid, M., Hammerle, A., Hampe, A., Haugum, S.V., Hederová, L., Heinesch, B., Helfter, C., Hepenstreich, D., Herberich, M., Herbst, M., Hermanutz, L., Hik, D.S., Höftrén, R., Homeier, J., Hörtnagl, L., Høye, T.T., Hrbacek, F., Hylander, K., Iwata, H., Antoni Jackowicz-Korczynski, M., Jactel, H., Järveoja, J., Jastrzębowski, S., Jentsch, A., Jiménez, J.J., Jónsdóttir, I.S., Jucker, T., Jump, A.S., Juszczak, R., Kanka, R., Kašpar, V., Kazakis, G., Kelly, J., Khuroo, A.A., Klemetsson, L., Klisz, M., Kljun, N., Knohl, A., Kobler, J., Kollár, J., Kotowska, M. M., Kovács, B., Kreyling, J., Lamprecht, A., Lang, S.I., Larson, C., Larson, K., Laska, K., le Maire, G., Leihy, R.I., Lens, L., Liljebladh, B., Lohila, A., Lorite, J., Loubet, B., Lynn, J., Macek, M., Mackenzie, R., Magliulo, E., Maier, R., Malfasi, F., Mális, F., Man, M., Manca, G., Manco, A., Manise, T., Manolaki, P., Marciniak, F., Matula, R., Clara Mazzolari, A., Medinets, S., Medinets, V., Meeussen, C., Merinero, S., de Cássia Guimarães Mesquita, R., Meusburger, K., Meysman, F.J.R., Michaletz, S.T., Milbau, A., Moiseev, D., Moiseev, P., Mondoni, A., Monfries, R., Montagnani, L., Moriana-Armandariz, M., Morra di Cella, U., Mörsdorf, M., Mosedale, J.R., Muffler, L., Muñoz-Rojas, M., Myers, J.A., Myers-Smith, I.H., Nagy, L., Nardino, M., Naujokaitis-Lewis, I., Newling, E., Nicklas, L., Niedrist, G., Niessner, A., Nilsson, M.B., Normand, S., Nosoito, M.D., Nouvellon, Y., Nuñez, M.A., Ogaya, R., Ogée, J., Okello, J., Olejnik, J., Eivind Olesen, J., Opedal, Ø., Orsenigo, S., Palaj, A., Pampuch, T., Panov, A.V., Pärtel, M., Pastor, A., Pauchard, A., Pauli, H., Pavelka, M., Pearce, W.D., Peichl, M., Pellissier, L., Penczykowski, R.M., Penuelas, J., Petit Bon, M., Petraglia, A., Phartyal, S.S., Phoenix, G.K., Pio, C., Pitacco, A., Pitteloud, C., Plichta, R., Porro, F., Portillo-Estrada, M., Poulénard, J., Poyatos, R., Prukushkin, A.S., Puchalka, R., Púscas, M., Radujković, D., Randall, K., Ratier Backes, A., Remmele, S., Remmers, W., Renault, D., Risch, A.C., Rixen, C., Robinson, S.A., Robroek, B.J.M., Rocha, A.V., Rossi, C., Rossi, G., Rouspard, O., Rubtsov, A.V., Saccione, P., Sagot, C., Sallo Bravo, J., Santos, C.C., Sarnel, J.M., Scharnweber, T., Schmeddes, J., Schmidt, M., Scholten, T., Schuchardt, M., Schwartz, N., Scott, T., Seeber, J., Cristina Segalin de Andrade, A., Seipel, T., Semenchuk, P., Senior, R.A., Serra-Diaz, J.M., Sewerniak, P., Shekhar, A., Sidenko, N.V., Siebicke, L., Siegwart Collier, L., Simpson, E., Siqueira, D.P., Sitková, Z., Six, J., Smiljanic, M., Smith, S.W., Smith-Tripp, S., Somers, B., Vedel Sørensen, M., João, L.L., Souza, J., Israel Souza, B., Souza Dias, A., Spasojevic, M.J., Speed, J.D.M., Spicher, F., Stanisci, A., Steinbauer, K., Steinbrecher, R., Steinwandter, M., Stelmkowsky, M., Stephan, J.G., Stiegler, C., Stoll, S., Svátek, M., Svoboda, M., Tagesson, T., Tanentzap, A.J., Tanneberger, F., Theurillat, J., Thomas, H.J.D., Thomas, A.D., Tielbörger, K., Tomaselli, M., Albert Treier, U., Trouillier, M., Dan Turtureanu, P., Tutton, R., Tyystjärvi, V.A., Ueyama, M.,

- Ujházy, K., Ujházyová, M., Uogintas, D., Urban, A.V., Urban, J., Urbaniak, M., Ursu, T., Primo Vaccari, F., Van de Vondel, S., van den Brink, L., Van Geel, M., Vandvik, V., Vangansbeke, P., Varlagin, A., Veen, G.F., Veenendaal, E., Venn, S.E., Verbeeck, H., Verbruggen, E., Verheijen, F.G.A., Villar, L., Vitale, L., Vittoz, P., Vives-Inglá, M., von Oppen, J., Walz, J., Wang, R., Wang, Y., Way, R.G., Wedegärtner, R.E.M., Weigel, R., Wild, J., Wilkinson, M., Wilmking, M., Wingate, L., Winkler, M., Wipf, S., Wohlfahrt, G., Xenakis, G., Yang, Y., Yu, Z., Yu, K., Zellweger, F., Zhang, J., Zhang, Z., Zhao, P., Ziemblínska, K., Zimmermann, R., Zong, S., Zyryanov, V.I., Nijs, I., Lenoir, J., 2021b. Global maps of soil temperature. *Glob. Change Biol.* gcb.16060. <https://doi.org/10.1111/gcb.16060>.
- Lenoir, J., Gril, E., Durrieu, S., Horen, H., Laslier, M., Lembrechts, J.J., Zellweger, F., Alleaume, S., Brasseur, B., Buridant, J., Dayal, K., De Frenne, P., Gallet-Moron, E., Marrec, R., Meeussen, C., Rocchini, D., Van Meerbeek, K., Decocq, G., 2022. Unveil the unseen: using LiDAR to capture time-lag dynamics in the herbaceous layer of European temperate forests. *J. Ecol.* 110, 282–300. <https://doi.org/10.1111/1365-2745.13837>.
- Lenoir, J., Hattab, T., Pierre, G., 2017. Climatic microrefugia under anthropogenic climate change: implications for species redistribution. *Ecography* 40, 253–266. <https://doi.org/10.1111/ecog.02788>.
- Lindenmayer, D., Blanchard, W., McBurney, L., Bowd, E., Youngentob, K., Marsh, K., Taylor, C., 2022. Stand age related differences in forest microclimate. *For. Ecol. Manag.* 510, 120101 <https://doi.org/10.1016/j.foreco.2022.120101>.
- Ma, L., Gu, X., Wang, B., 2017. Correction of outliers in temperature time series based on sliding window prediction in meteorological sensor network. *Information* 8, 60. <https://doi.org/10.3390/info8020060>.
- Macek, M., Kopecký, M., Wild, J., 2019. Maximum air temperature controlled by landscape topography affects plant species composition in temperate forests. *Landscape Ecol.* 34, 2541–2556. <https://doi.org/10.1007/s10980-019-00903-x>.
- Maclean, I.M.D., 2020. Predicting future climate at high spatial and temporal resolution. *Glob. Change Biol.* 26, 1003–1011. <https://doi.org/10.1111/gcb.14876>.
- Maclean, I.M.D., Duffy, J.P., Haesen, S., Govaert, S., De Frenne, P., Vanneste, T., Lenoir, J., Lembrechts, J.J., Rhodes, M.W., Van Meerbeek, K., 2021. On the measurement of microclimate. *Methods Ecol. Evol.* 12, 1397–1410. <https://doi.org/10.1111/2041-210X.13627>.
- Maclean, I.M.D., Klings, D.H., 2021. Microclim: a mechanistic model of above, below and within-canopy microclimate. *Ecol. Model.* 451, 109567 <https://doi.org/10.1016/j.ecolmodel.2021.109567>.
- Maclean, I.M.D., Mosedale, J.R., Bennie, J.J., 2019. Microclima: an R package for modelling meso- and microclimate. *Methods Ecol. Evol.* 10, 280–290. <https://doi.org/10.1111/2041-210X.13093>.
- Meeussen, C., Govaert, S., Vanneste, T., Bollmann, K., Brunet, J., Calders, K., Cousins, S. A.O., De Pauw, K., Diekmann, M., Gasperini, C., Hedwall, P.-O., Hylander, K., Iacopetti, G., Lenoir, J., Lindmo, S., Orczewska, A., Ponette, Q., Plue, J., Sanczuk, P., Selvi, F., Spicher, F., Verbeeck, H., Zellweger, F., Verheyen, K., Vangansbeke, P., De Frenne, P., 2021. Microclimatic edge-to-interior gradients of European deciduous forests. *Agric. For. Meteorol.* 311, 108699 <https://doi.org/10.1016/j.agrformet.2021.108699>.
- ONF, 2012. Révision d'Aménagement Forestier 2012–2031. Forêt Domaniale de Compiègne.
- Pincebourde, S., Salle, A., 2020. On the importance of getting fine-scale temperature records near any surface. *Glob. Change Biol.* 26, 6025–6027. <https://doi.org/10.1111/gcb.15210>.
- Rita, A., Bonanomi, G., Allevato, E., Borghetti, M., Cesarano, G., Mogavero, V., Rossi, S., Saulino, L., Zotti, M., Saracino, A., 2021. Topography modulates near-ground microclimate in the Mediterranean *Fagus sylvatica* treeline. *Sci. Rep.* 11, 8122. <https://doi.org/10.1038/s41598-021-87661-6>.
- Scheffers, B.R., Edwards, D.P., Diesmos, A., Williams, S.E., Evans, T.A., 2014. Microhabitats reduce animal's exposure to climate extremes. *Glob. Change Biol.* 20, 495–503. <https://doi.org/10.1111/gcb.12439>.
- Song, Y., Zhou, D., Zhang, H., Li, G., Jin, Y., Li, Q., 2013. Effects of vegetation height and density on soil temperature variations. *Chin. Sci. Bull.* 58, 907–912. <https://doi.org/10.1007/s11434-012-5596-y>.
- Stickley, S.F., Fraterrigo, J.M., 2021. Understorey vegetation contributes to microclimatic buffering of near-surface temperatures in temperate deciduous forests. *Landscape Ecol.* 36, 1197–1213. <https://doi.org/10.1007/s10980-021-01195-w>.
- Terando, A.J., Youngsteadt, E., Meineke, E.K., Prado, S.G., 2017. Ad hoc instrumentation methods in ecological studies produce highly biased temperature measurements. *Ecol. Evol.* 7, 9890–9904. <https://doi.org/10.1002/ece3.3499>.
- Vinod, N., Slot, M., McGregor, I.R., Ordway, E.M., Smith, M.N., Taylor, T.C., Sack, L., Buckley, T.N., Anderson-Teixeira, K.J., 2023. Thermal sensitivity across forest vertical profiles: patterns, mechanisms, and ecological implications. *New Phytologist.* 237, 22–47. <https://doi.org/10.1111/nph.18539>.
- Woods, H.A., Dillon, M.E., Pincebourde, S., 2015. The roles of microclimatic diversity and of behavior in mediating the responses of ectotherms to climate change. *J. Therm. Biol.* 54, 86–97. <https://doi.org/10.1016/j.jtherbio.2014.10.002>.
- Yu, Q., Acheampong, M., Pu, R., Landry, S.M., Ji, W., Dahigamuwa, T., 2018. Assessing effects of urban vegetation height on land surface temperature in the City of Tampa, Florida, USA. *Int. J. Appl. Earth Observ. Geoinform.* 73, 712–720. <https://doi.org/10.1016/j.jag.2018.08.016>.
- Yue, W., Xu, J., Tan, W., Xu, L., 2007. The relationship between land surface temperature and NDVI with remote sensing: application to Shanghai Landsat 7 ETM+ data. *Int. J. Remote Sens.* 28, 3205–3226. <https://doi.org/10.1080/01431160500306906>.
- Zellweger, F., Coomes, D., Lenoir, J., Depauw, L., Maes, S.L., Wulf, M., Kirby, K.J., Brunet, J., Kopecký, M., Mális, F., Schmidt, W., Heinrichs, S., den Ouden, J., Jaroszewicz, B., Buyse, G., Spicher, F., Verheyen, K., De Frenne, P., 2019. Seasonal drivers of understorey temperature buffering in temperate deciduous forests across Europe. *Glob. Ecol. Biogeogr.* 28, 1774–1786. <https://doi.org/10.1111/gcb.12991>.